

# Improved Crosstalk Modeling with Applications to Noise Constrained Interconnect Optimization \*

Jason Cong, David Zhigang Pan and Prasanna V. Srinivas<sup>†</sup>

Department of Computer Science, University of California, Los Angeles, CA 90095

<sup>†</sup> Magma Design Automation, Inc., 2 Results Way, Cupertino, CA 95014

## Abstract

*This paper presents a highly accurate yet efficient crosstalk noise model, the 2- $\pi$  model, and applies it to interconnect optimizations for noise reduction. Compared to previous crosstalk noise models with similar complexity, our 2- $\pi$  model takes into consideration many key parameters, such as coupling locations (near-driver or near-receiver) and the coarse distributed RC characteristics for the victim net. Thus, it is very accurate (less than 6% error on average compared with HSPICE simulations). Moreover, our model provides simple closed-form expressions for both peak noise amplitude and noise width. It is therefore very useful to guide noise-aware layout optimizations. In particular, we demonstrate its effectiveness in two applications: (i) optimization rule generation for noise reduction using various interconnect optimization techniques; (ii) simultaneous wire spacing to multiple nets for noise constrained area minimization.*

## 1 Introduction

In deep sub-micron (DSM) circuit designs, the coupling capacitance between adjacent nets has become a dominant component as taller and narrower wires are now placed closer to each other [1]. The coupling capacitance not only leads to excessive signal delays, but also causes potential logic malfunctions. The latter problem is especially serious for designs with high clock frequencies, low supply voltages, and usage of dynamic logic since they have low noise margin. To make sure a final layout to be noise immune, accurate yet efficient noise models are needed to guide interconnect optimizations at various stages.

In recent years, a number of researchers have worked on crosstalk noise modeling for layout optimizations. In [2], a simple peak noise formula was obtained by modeling each aggressor and victim net by an L-type RC circuit, under the *step* input assumption for aggressor nets. Later, [3, 4, 5] extended [2] to consider a *saturated ramp* input, or a Pi-type lumped RC circuit. Most of these models, however, did not consider distributed RC network, which is needed in DSM designs. In [6], an elegant Elmore-delay like peak noise model was obtained for general RC trees, and it guarantees to be an upper bound. However, [6] assumed an *infinite* (i.e., *non-saturated*) ramp input. Thus, it may significantly over-estimate the peak noise, especially for large victim nets and small aggressor transition times (very likely in DSM). In fact, the peak noise obtained from [6] may even be larger than the supply voltage. Recent work in [5] can handle distributed RC network and saturated ramp input. But it can be shown that [5] has up to 100% over estimation compared to the model in [6] when the aggressor transition time is much larger than the victim net delay (see more detailed explanation in Section 2).

In this paper, we develop a much improved crosstalk noise model, called the 2- $\pi$  model. It overcomes major drawbacks of existing models by taking into consideration many key parameters,

such as the aggressor slew at the coupling location, the coupling location at the victim net (near-driver or near-receiver), and the coarse distributed RC characteristics for victim net. Our model is very accurate, with less than 5% error on average compared with HSPICE simulations. Moreover, it enjoys simple *closed-form* expressions for both *peak noise* and *noise width* and provides very clear physical meaning for key noise contribution terms. All these characteristics of our 2- $\pi$  model make it ideal to guide noise-aware layout optimizations *explicitly*.

The rest of this paper is organized as follows. Section 2 presents the 2- $\pi$  model, its analytical solutions, and the validation by HSPICE simulations. Then, we demonstrate the effectiveness of our 2- $\pi$  model in noise constrained interconnect optimizations, followed by the conclusions in Section 4. Due to the space limitation, we leave some details of this paper in [7] which interested readers can refer to.

## 2 The 2- $\pi$ Crosstalk Noise Model

In this section, we first present the 2- $\pi$  model and the analytical solutions of its two key noise metrics (i.e., peak noise and noise width). We then extend the 2- $\pi$  model to handle general RC trees, and show experimental results to validate the model.

### 2.1 2- $\pi$ Model and its Analytical Solutions

For simplicity, we first explain our 2- $\pi$  model for the case where the victim net is an RC line. We will extend the 2- $\pi$  model to a general RC tree in Section 2.2. For a victim net with some aggressor nearby, as shown in Figure 1 (a), let the aggressor voltage pulse at the coupling location be a saturated ramp input with transition time (i.e., slew) being  $t_r$ , and the interconnect length of the victim net before the coupling, at the coupling and after the coupling be  $L_s$ ,  $L_c$  and  $L_e$ , respectively.

The 2- $\pi$  type reduced RC model is generated as shown in Figure 1 (b) to compute the crosstalk noise at the receiver. It is called 2- $\pi$  model because the victim net is modeled as 2- $\pi$  type RC circuits, one before the coupling and one after the coupling. The victim driver is modeled by effective resistance  $R_d$ . Other RC parameters  $C_x$ ,  $C_1$ ,  $R_s$ ,  $C_2$ ,  $R_e$ , and  $C_L$  are computed from the geometric information from Figure 1 (a) in the following manner. The coupling node (node 2) is set to be the center of the coupling portion of the victim net, i.e.,  $L_s + L_c/2$  from the source. Let the upstream and downstream interconnect resistance/capacitance at Node 2 be  $R_s/C_s$  and  $R_e/C_e$ , respectively. Then capacitance values are set to be  $C_1 = C_s/2$ ,  $C_2 = (C_s + C_e)/2$  and  $C_L = C_e/2 + C_l$ . Compared with [2, 3] which only used one lumped RC for the victim net, it is obvious that our 2- $\pi$  model can model the *coarse* distributed RC characteristics.

Since we consider only those *key* parameters, the resulting 2- $\pi$  model can be solved analytically (see [7] for details). Then using the dominant-pole approximation similar to [8, 4, 9], we have the following voltage waveform (in the  $s$ -domain) at the victim net

\*This work is partially supported by Semiconductor Research Corporation under Contract 98-DJ-605. Part of the work was performed while David Pan worked as a summer intern at Magma in 1999.

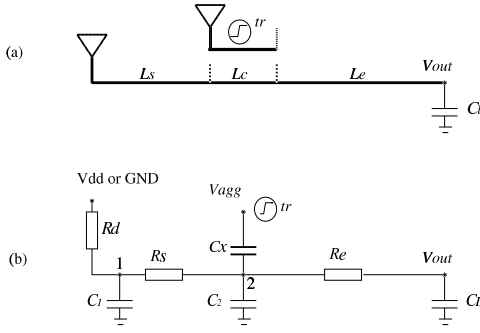


Figure 1: (a) The layout of a victim net and an aggressor above it. (b) The 2- $\pi$  crosstalk noise model.

sink (for a saturated aggressor input with transition time  $t_r$ , whose Laplace transformation is  $V_{agg}(s) = \frac{1-e^{-st_r}}{s^2 t_r}$ ):

$$V_{out}(s) = \frac{st_x}{st_v + 1} \cdot V_{agg}(s) = \frac{t_x(1 - e^{-st_r})}{st_r(st_v + 1)} \quad (1)$$

where the coefficients are

$$t_x = (R_d + R_s)C_x \quad (2)$$

$$t_v = (R_d + R_s)(C_x + C_2 + C_L) + (R_e C_L + R_d C_1). \quad (3)$$

It is interesting to observe that  $t_x$  is in fact the RC delay by the upstream resistance of the coupling element times the coupling capacitance, while  $t_v$  is the Elmore delay of the victim net.

Computing the inverse Laplace transform of (1), we can obtain the following simple time domain waveform

$$v_{out}(t) = \begin{cases} \frac{t_x}{t_r}(1 - e^{-t/t_v}) & 0 \leq t \leq t_r \\ \frac{t_x}{t_r}(e^{-(t-t_r)/t_v} - e^{-t/t_v}) & t > t_r \end{cases} \quad (4)$$

It is easy to verify that in the above noise expression,  $v_{out}$  monotonically increases at  $0 \leq t \leq t_r$ , and monotonically decreases at  $t > t_r$ . Thus, the peak noise will be at  $t = t_r$ , and its value is

$$v_{max} = \frac{t_x}{t_r}(1 - e^{-t_r/t_v}). \quad (5)$$

The above peak noise formula from the 2- $\pi$  model can be degenerated to some special cases to encapsulate noise models derived in previous works. As  $t_r \rightarrow 0$  (i.e., a step input),  $v_{max} \rightarrow \frac{t_x}{t_v}$ , which is in the same form as in [2] (without interconnect resistance) and [5] (with interconnect resistance). In the case of  $t_r \gg t_v$  (actually  $t_r > 3t_v$  is enough),  $v_{max} \rightarrow \frac{t_x}{t_r}$ , which is in the same form as [6].

It is also interesting to compare with the recent work by [5], where the peak noise with saturated ramp input can be written as  $v'_{max} = \frac{t_x}{t_v + t_r/2}$ . Although obtained from a totally different approach,  $v'_{max}$  from [5] is indeed a first-order approximation of our  $v_{max}$  in (5), since

$$\frac{t_x}{t_r}(1 - e^{-t_r/t_v}) = \frac{t_x}{t_v} \left[ 1 - \frac{1}{2} \frac{t_r}{t_v} + \dots \right] \quad (6)$$

$$\approx \frac{t_x}{t_v} \frac{1}{1 + \frac{1}{2} \frac{t_r}{t_v}} = \frac{t_x}{t_v + t_r/2} \quad (7)$$

However, such approximation is only valid when  $t_r < t_v$ . It will be much off when  $t_r \gg t_v$ , since it throws away larger terms. This explains why  $v'_{max}$  in [5] gives twice peak noise of that in [6] when

$t_r \gg t_v$ , i.e., 100% over estimation. It also explains the results in Table II of [5] that as  $t_r$  gets larger (from 100ps to 500ps), the average error of peak noise expression from [5] gets larger (from 6% to 10%).

Peak noise amplitude  $v_{max}$  is not the only metric to characterize noise. Under some circumstance, even the peak noise exceeds certain threshold voltage, a receiver may still be noise immune. This can be characterized by some noise amplitude versus width plots. The noise width is defined as follows.

**Definition 1 Noise Width:** Given certain threshold voltage level  $v_t$ , the noise width for a noise pulse is defined to be the length of time interval that noise spike voltage  $v$  is larger or equal to  $v_t$ .

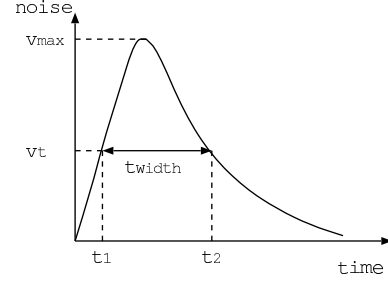


Figure 2: Illustration of the noise width.

From Eqn. (4), we can compute  $t_1$  and  $t_2$ , and thus the noise width

$$t_2 - t_1 = t_v \ln \left[ \frac{(t_x - t_r v_t)(e^{t_r/t_v} - 1)}{t_r v_t} \right] \quad (8)$$

In this paper, we set the threshold voltage  $v_t$  to be half of the peak noise voltage,  $v_t = v_{max}/2$ . Then, the noise width of (8) is simplified into

$$t_{width} = t_2 - t_1 = t_r + t_v \ln \left[ \frac{1 - e^{-2t_r/t_v}}{1 - e^{-t_r/t_v}} \right] \quad (9)$$

Note that  $t_x$  is cancelled out in (9). One can easily verify the following property for the noise width.

**Lemma 1** The noise width  $t_{width}$  is a monotonically increasing function of  $t_r$  and  $t_v$ , i.e.,  $\partial t_{width} / \partial t_r > 0$  and  $\partial t_{width} / \partial t_v > 0$ , and it is bounded by  $t_r < t_{width} < t_r + t_v \ln 2$ .

## 2.2 Extension to RC Trees

Our 2- $\pi$  model can be easily extended to a victim net in general RC tree structures. To compute the crosstalk noise at a certain sink (receiver)  $S_j$ , we build the corresponding 2- $\pi$  model as shown in Figure 3. It is similar to that shown in Figure 1, with the same upstream and downstream resistances. The only difference is that we now incorporate the lumped capacitance at each branch on the path from source to sink  $S_j$ , i.e.,  $C_{b1}, \dots, C_{bi}$ . We will add these  $C_{bi}$ 's into  $C_1, C_2$  or  $C_L$  in the following weighted manner:

- If a branch  $B_i$  is between the source and the coupling center, let its distance to the source be  $\alpha(L_s + L_c/2)$ . Then  $(1-\alpha)C_{bi}$  goes to  $C_1$  and  $\alpha C_{bi}$  goes to  $C_2$ .
- If a branch  $B_i$  is between the sink and the coupling center, let its distance to the sink be  $\beta(L_e + L_c/2)$ . Then  $(1-\beta)C_{bi}$  goes to  $C_L$  and  $\beta C_{bi}$  goes to  $C_2$ .

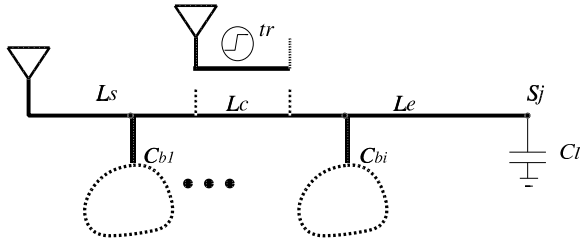


Figure 3: Extension of the 2- $\pi$  model for general RC trees.

Actually, it can easily be shown that in the resulting 2- $\pi$  model of multiple-pin nets,  $t_x$  is the same as that in 2-pin nets while  $t_v$  is still the Elmore delay from the source to sink  $S_j$ , but now with branching capacitances. The analytical solutions of the 2- $\pi$  model remain the same. Note that for a coupling element (e.g.,  $C_x$ ) not on the path from the source to sink  $S_j$  (i.e., coupling with some branching elements), the computation of  $t_x$  only takes  $C_x$ 's upstream resistance common to the path from the source to sink  $S_j$  (in the same principle as the Elmore delay computation).

As for the time complexity, given a 2- $\pi$  model, it only takes constant time to compute the peak noise and the noise width as we have the closed-form expressions for them. To reduce a distributed RC circuit to the 2- $\pi$  model, we only need a linear traversal of the victim net (to compute upstream/downstream interconnect resistance/capacitance at the coupling node and so on for  $t_x$  and  $t_v$ ), which can be done in linear time as well, the same as in [2, 6]. It is obvious to be the lower bound of the computational complexity for any reasonable noise model.

### 2.3 Validation of the 2- $\pi$ Model

The 2- $\pi$  model and its analytical peak noise as well as noise width expressions have been tested extensively and shown to work remarkably well compared to HSPICE simulations. To obtain high fidelity and to detect the corner scenarios, we run our 2- $\pi$  model and the models in [6] and [5] versus the HSPICE simulations on 1000 randomly generated circuits with realistic parameters in a 0.18 $\mu\text{m}$  technology (extracted based on NTRS'97 [1]). For the test circuits, the driver resistance  $R_d$  is from 20 to 2000  $\Omega$ , the loading capacitance  $C_l$  is from 4 to 50 fF, the length parameters  $L_s$ ,  $L_c$ , and  $L_e$  are from 1 to 2000  $\mu\text{m}$ , the wire width/spacing is either 1x or 2x minimum width/spacing, and the aggressor slew is from 10 to 500 ps. Our experiments show that the average errors for peak noise estimation using [6], [5] and our 2- $\pi$  model are 589%, 9%, and less than 4%, respectively. Table 1 summarizes the percentage of nets that fall into certain error ranges using the 2- $\pi$  model with closed-form peak noise and noise width expressions from (5) and (9) compared with those from running HSPICE simulations. We can see that using our model, both peak noise and noise width are within 4% error on average, and almost 95% nets have less than 10% errors.

Error range	$v_{max}$	$t_{width}$
within +/- 20%	99.9%	98.8%
within +/- 15%	95.8%	96.8%
within +/- 10%	93.5%	94.6%
within +/- 5%	83.1%	84.7%
Average error	3.7%	3.6%

Table 1: The percentage of nets that fall into the error ranges for peak noise ( $v_{max}$ ) and noise width ( $t_{width}$ ) from the 2- $\pi$  model.

We have also tested the 2- $\pi$  model on a set of randomly generated multiple-pin nets with general tree structures. Our experimental results show that our 2- $\pi$  model still works surprisingly well for general RC trees. Figure 4 shows the scatter diagram comparing the 2- $\pi$  model (y-axis) with HSPICE (x-axis) simulations for 20 randomly generated four-pin nets (i.e., with two branches). The experimental setting is the same as those for 2-pin nets. The branching wire length ranges from 1 to 2000  $\mu\text{m}$ . The branching location can be anywhere from driver to receiver. HSPICE simulations are performed on distributed RC networks by dividing each long wire into every 10 $\mu\text{m}$  segment. Again, for all test circuits, the 2- $\pi$  model gives very good estimation (close to the  $y = x$  line in the scatter diagram). The average errors for peak noise and noise width are just 4.3% and 5.89%, respectively.

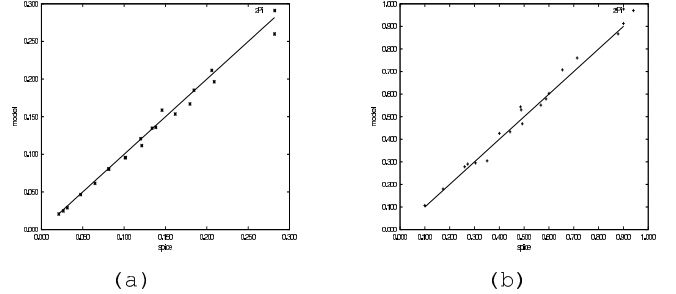


Figure 4: Comparison of 2- $\pi$  model versus HSPICE simulation for 20 randomly generated RC trees for (a) peak noise, (b) noise width.

## 3 Applications in Noise Reduction and Noise-Constrained Interconnect Optimization

Due to the high accuracy yet simple closed-form nature of the 2- $\pi$  model, we can use it in many different scenarios, from noise estimation/analysis to noise-aware interconnect optimizations. This section demonstrates the effectiveness of our model.

### 3.1 Some Optimization Rules for Noise Reduction

From the closed-form formulae of peak noise and noise width, we can perform parametric studies and obtain a set of optimization rules to guide effective noise reduction. The derivation and justification of these rules are in [7]. The following four rules are on the peak noise.

**Rule 1 (On Driver Sizing)** If  $R_s C_1 < R_e C_L$ , then sizing up the victim driver strength (i.e., reduce effective  $R_d$ ) will reduce peak noise. However, if  $R_s C_1 > R_e C_L$  and  $t_r \ll t_v$ , driver sizing will not help to reduce peak noise. In either situation, there is certain lower bound for peak noise that can be achieved by just doing driver sizing.

**Rule 2 (On Coupling Location)** During topology generation/routing of a noise-sensitive victim net, one shall avoid near-receiver coupling, especially to its strong aggressors.

**Rule 3 (On Shield Insertion)** The placement/insertion of non-aggressive (quiet) neighbors around a victim net will help to reduce the crosstalk noise. The preferred position for shield insertion is near a noise-sensitive net's receiver.

**Rule 4 (On Wire Sizing and Spacing)** Wire spacing is always an effective way to reduce noise, with an area penalty. For a given area constraint, wire spacing is usually more effective than wire sizing for crosstalk noise reduction.

Sometimes, a receiver may still be noise-immune even the peak noise exceeds certain threshold voltage. This can be characterized by some noise amplitude versus width plots, which can then be transformed into an *amplitude* (A) versus *amplitude-width* (AW) product (A-AW plot) [2]. This subsection reveals some interesting property on the noise amplitude-width product. From (5) and (9) the AW product can be written as

$$AW = (R_d + R_s)C_x \cdot f(x) \quad (10)$$

where  $f(x) = \frac{e^x - e^{-x}}{1 - e^{-x}} \ln \frac{e^x - e^{-x}}{1 - e^{-x}}$  and  $x = t_r/t_v$ . It can be verified that  $f(x) \in [\ln 2, 1]$ . Thus, we have the following important rule:

**Rule 5 (On Noise Amplitude-Width Product)** *The noise amplitude-width product has a lower bound of  $\ln 2(R_d + R_s)C_x$ , and an upper bound of  $(R_d + R_s)C_x$ . Other parameters such as  $C_1$ ,  $C_2$ ,  $R_e$ ,  $C_L$  only play a minor role in it. The effective ways to reduce AW are wire spacing, driver sizing and wire sizing.*

### 3.2 Simultaneous Wire Spacing for Multiple Nets

To further demonstrate the effectiveness of our  $2-\pi$  model, we apply it to a simultaneous wire spacing problem for multiple nets.

**Given:** (1) The initial layout of multiple nets and their noise constraints; (2) the minimum wire spacing between each coupling pair.

**Minimize:** The total area or equivalently, the total spacing between all nets.

**Subject to:** No noise violation for each net.

This problem may be formulated into some nonlinear programming problem under simple formula-based capacitance models. But in DSM designs, table-based capacitance model is usually required for adequate accuracy, which makes the problem difficult to solve due to lack of analytical expressions (possible non-convexity, etc.). Thus, we propose a simple but effective *sensitivity-based spacing algorithm* (SBSA) to solve it. The *noise reduction sensitivity*  $\Delta v_{ij}$  at some spacing  $s_{ij}$  (between two adjacent nets  $i$  and  $j$ ) is defined to be the total noise reduction for those noise-violating receivers in nets  $i$  and  $j$ , due to some nominal spacing increase to  $s_{ij}$ , say  $\Delta s_{ij}$ . The algorithm starts from some initial layout. As long as there is noise violation, it checks each spacing that is a possible cause of the noise violation, compute its noise reduction sensitivity, and selects the one with the most effective noise reduction due to a nominal spacing increment. This procedure will be repeated until there is no noise violation.

We apply our SBSA to a 4-bit fully parallel bus of 1 mm long, with  $R_d = 180\Omega$ ,  $C_l = 23\text{fF}$ , wire width of  $0.44\mu\text{m}$ , and  $t_r = 50\text{ps}$ . The noise constraint is set to be  $0.2 V_{dd}$ . Table 2 lists the spacings between adjacent bus lines using SBSA. We compare the resulting spacings ( $s_{12}$  denotes the spacing between the first and the second bus line, and so on.  $TS$  denotes the total spacing) from our metrics with two other metrics [6] (Devgan) and [5] (Vittal). We list results under two different  $\Delta s$ ,  $0.33\mu\text{m}$  and  $0.11\mu\text{m}$ , respectively. It can be seen that using Devgan and Vittal models may lead to too conservative spacing by as much as 70% and 31%, respectively, due to their peak noise over-estimation. It is also interesting to see that, comparing with a straightforward equal spacing algorithm (i.e.,  $s_{12} = s_{23} = s_{34}$ , with the total spacing  $TS_{ES}$  at the last row of Table 2), the SBSA algorithm will use much less area, with area reduction by up to 11% (total spacing of  $5.28\mu\text{m}$  versus  $5.94\mu\text{m}$  for  $2-\pi$  model with  $\Delta s = 0.33\mu\text{m}$ ).

spacing ( $\mu\text{m}$ )	$\Delta s = 0.33\mu\text{m}$			$\Delta s = 0.11\mu\text{m}$		
	Devgan	Vittal	$2-\pi$	Devgan	Vittal	$2-\pi$
$s_{12}$	2.64	1.98	1.65	2.42	1.98	1.54
$s_{23}$	3.63	2.97	1.98	3.52	2.75	2.20
$s_{34}$	2.64	1.98	1.65	2.42	1.98	1.54
$TS$	8.91	6.93	5.28	8.36	6.71	5.28
$TS_{ES}$	8.91	6.93	5.94	8.58	6.93	5.61

Table 2: Spacing for noise control of a 4-bit bus, using different noise metrics.

## 4 Conclusion

We have developed in this work a much improved, closed form crosstalk noise model, with on average less than 6% error compared with HSPICE simulation, for both peak noise voltage and noise width estimations. Compared to existing models with similar complexity, our model has much better accuracy and it provides a unified view for them. We then apply our model to develop a set of interconnect optimization rules to guide noise-aware interconnect optimizations, including driver sizing, topology construction, shield insertion and wire spacing versus sizing to reduce peak noise. We also obtain a very interesting bound on the noise amplitude-width product and provide a simple, effective rule to reduce it. We then apply our model to a simultaneous wire spacing problem and show significant area saving due to our more accurate modeling. We expect that our  $2-\pi$  model will be useful in many other applications at various levels to guide noise-aware DSM circuit designs.

## Acknowledgments

The authors would like to thank Tim Burks from Magma Design Automation, Inc., for helpful discussions.

## References

- [1] Semiconductor Industry Association, *National Technology Roadmap for Semiconductors*, 1997.
- [2] A. Vittal and M. Marek-Sadowska, "Crosstalk reduction for VLSI," *IEEE Trans. on Computer-Aided Design of Integrated Circuits and Systems*, vol. 16, pp. 290–98, 1997.
- [3] S. Nakagawa, D. M. Sylvester, J. McBride, and S.-Y. Oh, "On-chip cross talk noise model for deep-submicrometer ulsi interconnect," *Hewlett-Packard Journal*, vol. 49, pp. 39–45, Aug. 1998.
- [4] A. B. Kahng, S. Muddu, and D. Vidhani, "Noise and delay uncertainty studies for coupled rc interconnects," in *IEEE International ASIC/SOC Conference*, pp. 3–8, 1999.
- [5] A. Vittal, L. Chen, M. Marek-Sadowska, K.-P. Wang, and S. Yang, "Crosstalk in VLSI interconnections," *IEEE Trans. on Computer-Aided Design of Integrated Circuits and Systems*, vol. 18, no. 2, pp. 1817–24, 1999.
- [6] A. Devgan, "Efficient coupled noise estimation for on-chip interconnects," in *Proc. Int. Conf. on Computer Aided Design*, pp. 147–153, 1997.
- [7] J. Cong, D. Z. Pan, and P. V. Srinivas, "An improved crosstalk model and its applications," Tech. Rep. 200013, UCLA CS Dept, 2000.
- [8] M. Kuhlmann, S. Sapatnekar, and K. Parhi, "Efficient crosstalk estimation," in *Proc. IEEE International Conference on Computer Design*, pp. 266–272, 1999.
- [9] E. Acar, A. Odabasioglu, M. Celik, and L. Pileggi, "S2p: a stable 2-pole RC delay and coupling noise metric IC interconnects," in *Proceedings 9th Great Lakes Symposium on VLSI*, pp. 60–3, 1999.